Phase transitions and equations of state of alkaline earth fluorides CaF_2, SrF_2, and BaF_2 to Mbar pressures

Susannah M. Dorfman,[1] Fuming Jiang,[1,*] Zhu Mao,[1,†] Atsushi Kubo,[1,‡] Yue Meng,[2] Vitali B. Prakapenka,[3] and Thomas S. Duffy[1]

[1]*Department of Geosciences, Princeton University, Princeton, New Jersey 08544, USA*

[2]*High-Pressure Collaborative Access Team, Carnegie Institution of Washington, 9700 South Cass Avenue, Argonne, Illinois 60439, USA*

[3]*Consortium for Advanced Radiation Sources, University of Chicago, 9700 South Cass Avenue, Argonne, Illinois 60439, USA*

(Received 11 March 2010; revised manuscript received 28 April 2010; published 27 May 2010)

Phase transitions and equations of state of the alkaline earth fluorides CaF_2, SrF_2, and BaF_2 were examined by static compression to pressures as high as 146 GPa. Angle-dispersive x-ray diffraction experiments were performed on polycrystalline samples in the laser-heated diamond-anvil cell. We confirmed that at pressures less than 10 GPa all three materials undergo a phase transition from the cubic ($Fm\bar{3}m$) fluorite structure to the orthorhombic (*Pnam*) cotunnite-type structure. This work has characterized an additional phase transition in CaF_2 and SrF_2: these materials were observed to transform to a hexagonal ($P6_3/mmc$) Ni_2In-type structure between 63–79 GPa and 28–29 GPa, respectively, upon laser heating. For SrF_2, the Ni_2In-type phase was confirmed by Rietveld refinement. Volumes were determined as a function of pressure for all high-pressure phases and fit to the third-order Birch-Murnaghan equation of state. For CaF_2 and SrF_2, the fluorite-cotunnite transition results in a volume decrease of 8–10 %, while the bulk modulus of the cotunnite-type phase is the same or less than that of the fluorite phase within uncertainty. For all three fluorides, the volume reduction associated with the further transition to the Ni_2In-type phase is ~5%. The percentage increase in the bulk modulus (ΔK) across the transition is greater when the cation is smaller. While for BaF_2, ΔK is 10–30 %, ΔK values for SrF_2 and CaF_2 are 45–65 % and 20–40 %. Although shock data for CaF_2 have been interpreted to show a transition to a highly incompressible phase above 100 GPa, this is not consistent with our static equation of state data.

DOI: 10.1103/PhysRevB.81.174121 PACS number(s): 61.50.Ks, 62.50.−p, 64.30.Jk, 91.60.Gf

I. INTRODUCTION

The AX_2 family includes a variety of compounds of interest in geosciences, materials science, and condensed-matter physics that exhibit extensive polymorphism dependent on ionic size, electronic properties, and pressure.[1] One common highly coordinated polymorph is the fluorite structure, which is the stable polymorph at ambient conditions for the alkaline earth fluorides CaF_2, SrF_2, and BaF_2. Fluorides are widely used as windows and lenses, optical coatings, scintillators, and luminescent materials.[2] At high pressures, CaF_2 has been proposed as a pressure calibration standard.[3,4] The high coordination of the alkaline earth fluorides at ambient conditions can be analogous to the structure of lower coordination AX_2 compounds at high pressure, including oxides relevant to geoscience and planetary science.[1] High-pressure studies on CaF_2, SrF_2, and BaF_2 have addressed band structure,[5–11] metallization,[5–9,11,12] optical properties,[5,6,9,11] melting behavior,[13] shear strength,[14] phase transitions,[5,6,10,11,15–18] and elastic properties.[10,11,15,19–23] The relative simplicity of the AF_2 system makes it well suited for evaluating differences between theoretical and experimental studies of these properties.

The alkaline earth fluorides undergo a series of pressure-induced phase transitions to highly coordinated AX_2 structures. At ambient conditions, CaF_2, SrF_2, and BaF_2 all crystallize in the cubic fluorite structure ($Fm\bar{3}m$, $Z=4$), which consists of a cubic close-packed array of cations with anions occupying tetrahedral sites. Experiments have shown that these materials transform to the orthorhombic cotunnite-type structure (*Pnam*, $Z=4$) at 9 GPa, 5 GPa, and 3 GPa, respectively.[24–27] The cotunnite structure is characterized by anions in a distorted hexagonal-close-packed (hcp) lattice. The cations are situated within tricapped trigonal prisms with the three outer anions in the plane of the cation. An additional phase transition from the cotunnite phase to a hexagonal anti-Ni_2In-type phase ($P6_3/mmc$, $Z=2$) has been found experimentally in BaF_2 at 12 GPa by Leger *et al.*[16] The anti-Ni_2In-type structure is a subgroup of the cotunnite structure with an ideal hcp anion lattice. The higher-symmetry lattice incorporates two more anions in the plane of the cations, forming pentacapped prisms. The transition sequence from fluorite to cotunnite-type to Ni_2In-type thus involves an increase in the coordination number from 8 to 9 to 11. These structures are also common in oxides at higher pressures. Cotunnite-type phases have been synthesized for TiO_2,[28,29] SnO_2,[30] PbO_2,[31] ZrO_2,[32,33] HfO_2,[32,34] and CeO_2,[35] and *ab initio* theory predicts SiO_2 will transform to the cotunnite structure above 750 GPa.[36] Such high pressures are difficult to access experimentally, so information about the properties of high coordination phases of silica and other oxides must be derived either by theoretical methods or by experiments on analogs, such as fluorides.

As a model ionic system with useful physical properties, the alkaline earth fluorides have been extensively studied by *ab initio* and atomistic theoretical methods.[5–13,17–19] Theoretical studies have provided predictions of the phase transitions and equations of state for CaF_2,[5,7,10,11,19] SrF_2,[6,7,17] and BaF_2.[8,9,12,18] Although the transition to the cotunnite-type phase at high pressure is well known in CaF_2 and SrF_2, the

compressibility of these materials is poorly constrained. For CaF_2, theoretical predictions of the zero-pressure bulk modulus of the cotunnite phase span a wide range from 66 to 154 GPa, and thus it is not clear whether the transition from fluorite (K_0=82 GPa) to cotunnite involves a modest decrease or a large increase in the bulk modulus. Available experimental data[15] suggest a relatively high bulk modulus (K_0=170 GPa) for the cotunnite-type phase of CaF_2. The situation is similar for SrF_2, where theoretical predictions of K_0 for the cotunnite phase span a wide range, but in this case there is no experimental data for comparison.

At higher pressures, the transition to the Ni_2In-type phase previously found in BaF_2 (Ref. 16) has been predicted in CaF_2 and SrF_2. Theoretical studies[5,10,11] of CaF_2 predict transition pressures to the Ni_2In phase that vary between 68 and 278 GPa. For SrF_2, the transformation has recently been predicted to occur at about 46 GPa.[6] No experimental studies yet exist to compare with these theoretical findings. Existing theoretical studies[5,6,10,11] predict values of the zero-pressure bulk modulus for 11-coordinated Ni_2In-type SrF_2 and CaF_2 that are comparable or even lower than values for the eight-coordinated fluorite phase. Experimental data[12] on BaF_2 in a quasihydrostatic (He) pressure medium also yield a low bulk modulus for the Ni_2In phase in this composition, in contrast to earlier nonhydrostatic results.[16] Thus, these compounds appear to exhibit surprisingly high compressibilities for dense, highly coordinated high-pressure phases. These results stand in contrast to shock compression studies that suggest fluorides such as CaF_2 transform to remarkably incompressible phases above 100 GPa.[37,38]

In other systems such as dioxides, diborides, and dinitrides, highly coordinated AX_2 compounds have been synthesized at high pressure and are associated with low compressibilities. High-pressure phases of TiO_2,[28,29] ReB_2,[39] and IrN_2[40] have been examined as potential ultrahard or ultraincompressible materials. The cotunnite phase of TiO_2 has been reported to be both highly incompressible and hard with a zero-pressure bulk modulus of 294–431 GPa (Refs. 41–43) and a measured Vickers microhardness of 38 GPa.[41] The compressibility of corresponding fluoride phases is not yet well known.

In this work, we use x-ray diffraction in the laser-heated diamond-anvil cell (DAC) to investigate the equation of state and phase stability in CaF_2, SrF_2, and BaF_2 to Mbar pressures to provide new experimental constraints on the properties of high-pressure phases in this system. The results are used to explore the systematic high-pressure behavior of AX_2 fluorides and compare with theoretical predictions.

II. METHOD

Powder samples of CaF_2 (99.985% purity) and SrF_2 (99.99%) were obtained from Alfa Aesar and BaF_2 (99.99%) from Sigma-Aldrich. X-ray diffraction confirmed that each material was in the fluorite-type structure and no impurities or other phases were detectable. Zero-pressure volumes were measured to be 163.6(2) Å^3, 195.7(2) Å^3, and 238.3(2) Å^3 for CaF_2, SrF_2, and BaF_2, respectively.

High-pressure experiments were performed using synchrotron x-ray diffraction in a DAC. The samples were ground to a few micron grain size and mixed with 10–15 wt % platinum (99.9% purity, 0.5–1.2 μm particle size, Aldrich) as a laser absorber and pressure calibrant. A foil of the fluoride mixture was loaded into a symmetric DAC, sandwiched between two NaCl foils to provide a quasihydrostatic pressure medium and thermal insulation during laser heating.[44] For one CaF_2 sample, we used a pressurized gas loading system[45] to load a Ne medium, with a NaCl foil supporting the sample on one side.

For experiments at pressures up to about 65 GPa, we used diamond anvils with 300 μm culets, with the sample placed in a 150 μm hole in a stainless steel gasket. In higher-pressure experimental runs, we used 200 μm flat culet or 300/100 μm or 300/75 μm beveled culet diamond anvils. In these runs, we used rhenium gaskets with a 90 μm, 50 μm, or 25 μm sample chamber, respectively. Gaskets were preindented to 25 μm thickness before sample loading. Anvils were supported by either tungsten carbide seats with 50° conical holes or x-ray transparent cubic boron nitride seats with 33° conical holes.

Angle-dispersive x-ray diffraction with laser heating was performed at beamlines X17B3 of the National Synchrotron Light Source (NSLS) and 13-ID-D of the GSECARS sector and 16-ID-B of the HPCAT sector of the Advanced Photon Source (APS). At all facilities the x-ray beam was focused with a Kirkpatrick-Baez double mirror system. At X17B3, the x-ray beam size was approximately 20×30 μm, while at GSECARS, the beam size was 5×6 μm and at HPCAT, 5×10 μm. The detector at X17B3 was either an offline Fuji BAS2500 image plate or an online Mar345 image plate. At GSECARS and HPCAT we used a MarCCD charge-coupled device detector. The distance and orientation of the detector was calibrated using a CeO_2 standard; at X17B3, an Au standard was also used for confirmation and simultaneous wavelength calibration.

Table I lists all experimental runs reported in this study. We conducted both compression and decompression experiments. Laser annealing was required for equation of state measurements since the NaCl medium is not sufficient by itself to provide quasihydrostatic conditions. All samples were heated from both sides at high pressures with a Nd:YLF (neodymium:yttrium lithium fluoride) or Nd:YAG (neodymium:yttrium aluminum garnet) laser.[46,47] Temperatures were measured by spectroradiometry.[48] Heating was carried out to temperatures ranging from 1500 to 3000 K for typical durations of 20 min. For one CaF_2 run, we heated the sample with a Nd:YLF laser at the MIT Mineral Physics Laboratory, and then decompressed without additional heating at X17B3. After heating, Debye rings from fluoride samples were smooth, indicating little preferred orientation. Diffraction peak widths sharpened significantly due to heating: an unheated sample at 82 GPa showed a reduction in peak full width at half maximum of over 50% after heating.

Two-dimensional diffraction images were radially integrated using FIT2D software[49] to produce one-dimensional diffraction patterns. To obtain peak positions, widths, and intensities, patterns were fit with background-subtracted Voigt line shapes. Lattice parameters were refined for all data using UNITCELL.[50] Rietveld refinement of selected patterns was conducted using GSAS and EXPGUI software.[51,52]

TABLE I. Summary of experimental runs.

Material	Beamline	Detector	Culet, gasket hole (μm)	Pressure range (GPa)	P-T path
CaF_2	APS GSECARS 13-ID-D	CCD	200, 90	13–95	Compression with laser heating above 82 GPa
CaF_2	APS GSECARS 13-ID-D	CCD	300, 150	4–64	Compression with laser heating above 45 GPa
CaF_2	NSLS X17B3	Image plate	200, 90	56–84	Heating, cold decompression
CaF_2	APS GSECARS 13-ID-D	CCD	300/75, 25	90–146	Heated compression
CaF_2	APS GSECARS 13-ID-D	CCD	300, 150	15–60	Heated compression in Ne medium
SrF_2	NSLS X17B3	Image plate	200, 90	58–89	Heated compression
SrF_2	APS GSECARS 13-ID-D	CCD	300, 150	9–64	Heated compression, heated decompression
BaF_2	APS HPCAT 16-ID-B	CCD	300/100, 50	4–133	Heated compression

Pressure was determined from the equation of state of platinum.[53] Measured lattice strains in Pt were also used to evaluate differential stress, t, following the theory by Singh.[54] In the presence of differential stress, the elastic anisotropy S of Pt results in systematic variations in diffraction lines as a function of lattice plane, hkl. For a pair of reflections at similar diffraction angle, 2θ, Singh's equations for lattice strain in a cubic crystal in an axial, angle-dispersive geometry can be approximated[55] as

$$\frac{a_{hkl}-a_{hkl^*}}{a_0} \approx -St[1-3\cos^2(90^\circ-\theta_{hkl})][\Gamma(hkl)-\Gamma(hkl^*)],$$

where a is the lattice parameter for a given hkl, a_0 is the lattice parameter at ambient pressure, and Γ is $(h^2k^2+k^2l^2+l^2h^2)/(h^2+k^2+l^2)^2$. The angular proximity and strong intensity of the Pt 111 and 200 peaks make them ideal for this analysis. The elastic anisotropy of Pt as a function of pressure was taken from *ab initio* calculations[56] which we fit to an exponential relation: $S(P)=0.0012+0.0027\exp(-0.0058P)$, where P is in gigapascal and S in inverse gigapascal. This analysis showed that laser annealing reduced differential stress to less than 1 GPa in Pt. Only annealed data were used in equation of state fits.

III. RESULTS

A. Phase identification

Representative high-pressure diffraction patterns for CaF_2, SrF_2, and BaF_2 are shown in Figs. 1–3. All patterns can be indexed to the cubic fluorite phase, the orthorhombic cotunnite-type phase,[20,24,25] or the hexagonal Ni_2In-type phase.[16] Representative comparisons of measured and fit d spacings for the cotunnite and Ni_2In phases of CaF_2 are shown in Tables II and III. No other phases were observed up to 146 GPa in CaF_2, 89 GPa in SrF_2, and 133 GPa in BaF_2, either at 300 K or during laser heating at 1500–2500 K. For BaF_2, a sample heated to 3000 K at 111 GPa showed additional weak peaks that were preserved up to 133 GPa with further heating and may be due to a reaction between the sample and the surrounding materials.

For all samples, the fluorite-cotunnite phase transition was observed to occur without heating. The observed transition pressure for our room-temperature compression of CaF_2 and SrF_2 is higher than that in other studies;[12,15,16,24–27] this reflects variations in metastable behavior under different degrees of differential stress. During initial pressurization of the DAC, BaF_2 was compressed to 3.8 GPa, and the transition from fluorite to cotunnite-type was already completed at this pressure.

Our study has experimentally identified the Ni_2In-type phase in SrF_2 and CaF_2. In SrF_2, the orthorhombic cotunnite-type phase transformed to the hexagonal Ni_2In-type phase upon compression at 36 GPa with heating to about 1500 K. The new phase was maintained upon decompression with heating down to 29 GPa. At 28 GPa, diffraction patterns measured during heating to 1500–2000 K exhibited the Ni_2In-type phase, but upon quench the SrF_2 sample had returned to the cotunnite structure. This is evidence that the cotunnite to Ni_2In-type transition has a negative Clapeyron slope but uncertainty in temperature measurement makes the slope difficult to quantify. Another SrF_2 sample compressed directly to 58 GPa without heating displayed broad diffraction peaks consistent with the Ni_2In-type phase that sharpened with subsequent heating. CaF_2 transformed from the cotunnite-type phase to the Ni_2In-type phase at 79 GPa with

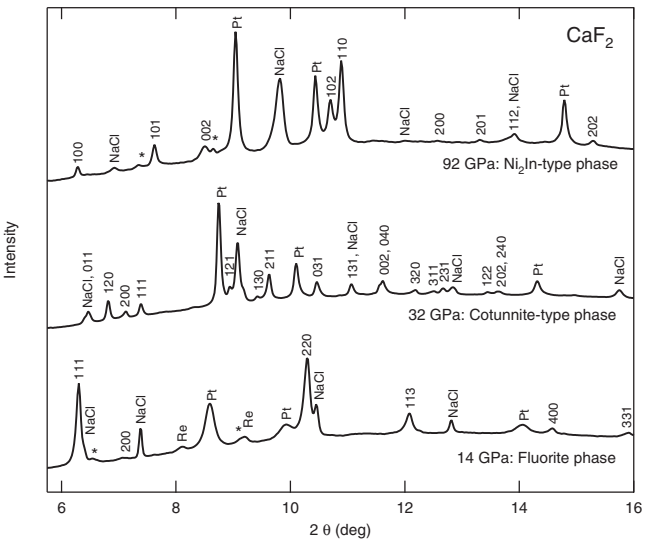

FIG. 1. Representative x-ray diffraction patterns for CaF_2. Peaks labeled with asterisks in fluorite and Ni_2In-type patterns are from minor amounts of the cotunnite-type phase.

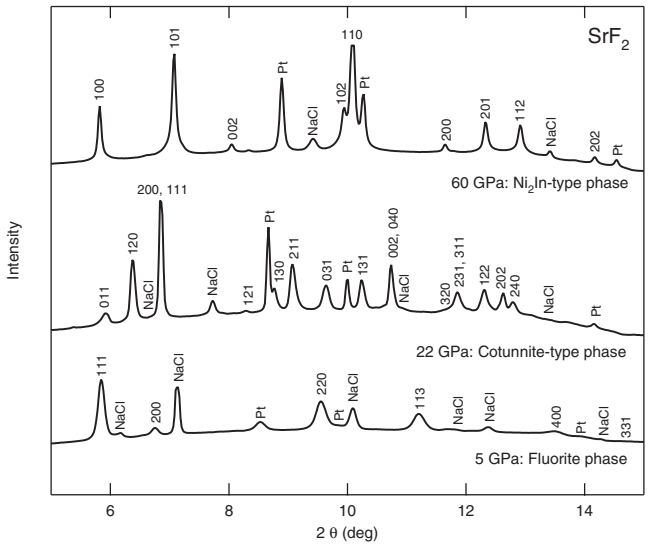

FIG. 2. Representative x-ray diffraction patterns for SrF_2.

heating to about 2000 K. Upon decompression without heating, diffraction peaks remained sharp to 72 GPa but broadened significantly at lower pressures and the sample appeared to become partially amorphous. Laser heating at 63 GPa produced the cotunnite phase. For all compositions, the Ni_2In-type phase could not be recovered to ambient pressure. Based on our temperature-quenched diffraction patterns, these experiments constrain the cotunnite-Ni_2In-type transition pressure at 300 K to 28–29 GPa for SrF_2 and 63–79 GPa for CaF_2.

The transition from the cotunnite-type to Ni_2In-type phase in CaF_2 and SrF_2 has also been investigated at 0 K by theoretical studies using density-functional theory.[5,6,10,11] For CaF_2, our results are more consistent with the predicted transition pressure found by Wu *et al.*[5] (68–72 GPa) than by Shi *et al.*[10] (105 GPa) or Cui *et al.*[11] (278 GPa). For SrF_2, the transition occurred at pressures lower than predicted (45.6 GPa).[6] Some of the differences in phase-transition pressures between experiment and theory may reflect thermal effects. While the negative Clapeyron slope observed does support higher transition pressures at 0 K than at 300 K, this is unlikely to account for more than a few gigapascal difference. More critical to the accuracy of these predicted transition pressures is the similarity between the cotunnite and Ni_2In-type phases and their calculated enthalpies. A small enthalpy difference between these structures over a wide pressure range as observed in these calculations makes the transition pressure particularly sensitive to error in computational parameters. Such a small enthalpy difference would also increase the dependence of experimental results on temperature, differential stress, and kinetics.

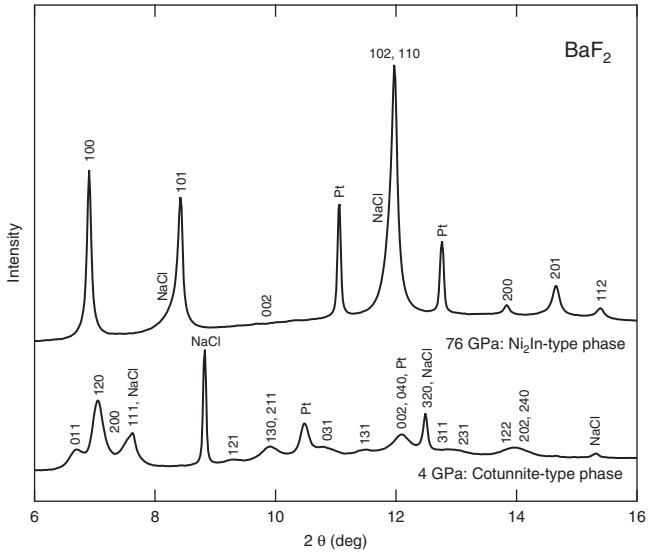

FIG. 3. Representative x-ray diffraction patterns for BaF_2.

The Ni_2In-type structure of SrF_2 at 58.4 GPa was confirmed by full profile refinement (Fig. 4). Except for a broad unknown peak with a 2θ value of approximately 8°, all peaks could be indexed as NaCl B2 phase, Pt, or SrF_2 in the Ni_2In structure. Lattice parameters, phase fractions, peak shape parameters, and spherical harmonic terms were refined for all phases. As all atoms are in special positions, no refinement of atomic positions was necessary. The texture index was 1 for NaCl, 1.11 for Pt, and 3.47 for SrF_2 indicating substantial preferred orientation, with the (001) plane aligned normal to the compression direction. The refinement yielded lattice parameters $a=3.8130(2)$ Å and $c=4.7788(21)$ Å, and a volume of 60.171(26) Å^3, consistent with values obtained by individual peak fitting to within 0.1%.

B. Equation of state

Unit-cell volumes for CaF_2, SrF_2, and BaF_2 were fit to a third-order Birch-Murnaghan equation of state and the results are shown in Fig. 5 and Tables IV and V. It is well known that volume compression data may suffer from tradeoffs in constraining the three zero-pressure parameters of the equation of state, volume V_0, bulk modulus K_0, and pressure derivative of the bulk modulus K_0'. In order to better constrain K_0, we fixed V_0 or K_0'. Most of the uncertainty in the fit comes from poor constraint on V_0. Fixing the zero-pressure volume of the high-pressure phases to various values based on previous experimental or theoretical results (Tables IV and V) results in a range of values for K_0 and K_0'. This range illustrates the error in our constraint of these zero-pressure equation of state parameters due to parameter trade-offs. Alternatively, K_0' may be fixed to a reasonable value based on previous work. Previous experimental and theoretical work on CaF_2, SrF_2, and BaF_2 found that K_0' is 4.67–4.7 for all phases of BaF_2,[12] 4.75 for the fluorite phase of SrF_2,[21] and 4.38–4.83 for all phases of CaF_2,[11,22] suggesting that K_0' may have little variation with structure or cation for the alkaline earth fluorides. We therefore chose a K_0' of 4.7 when using a fixed value for this parameter in our fits.

1. Cotunnite-type phase

The results of equation of state fits for the cotunnite phases of CaF_2 and SrF_2 are compared with earlier studies in Table IV. With K_0' fixed at 4.7, the zero-pressure volumes of the cotunnite-type phases of CaF_2 and SrF_2 are 6–10 % less than V_0 of the corresponding fluorite phases at ambient con-

TABLE II. Observed and calculated d spacings for the cotunnite-type phase of CaF_2 at 35 GPa and 300 K. These peaks are fit to an orthorhombic unit cell with $a=5.3869(10)$ Å, $b=6.5955(13)$ Å, $c=3.3149(7)$ Å, and $V=117.78(3)$ Å^3.

h	k	l	d_{obs} (Å)	d_{calc} (Å)	Δd (Å)	Intensity (%)
0	1	1	2.96239	2.96183	0.00056	47
1	2	0	2.81191	2.81259	−0.00068	82
2	0	0	2.69359	2.69347	0.00012	26
1	1	1	2.59449	2.5954	−0.00091	48
1	2	1	2.14467	2.14463	0.00004	50
2	0	1	2.09014	2.0904	−0.00026	31
1	3	0	2.03592	2.03552	0.0004	12
2	1	1	1.99243	1.99271	−0.00028	100
0	3	1	1.83303	1.83218	0.00085	63
1	3	1	1.73396	1.73459	−0.00063	48
3	2	0	1.57698	1.57702	−0.00004	16
3	1	1	1.53659	1.5355	0.00109	10
2	3	1	1.51534	1.51491	0.00043	23
1	2	2	1.42777	1.42794	−0.00017	9

ditions. For CaF_2, this is consistent with density-functional theory[5,10,11] and with the measured volume of cotunnite-type CaF_2 synthesized at ambient conditions[57] or recovered from shock compression.[58] It is also consistent with the volume difference between cotunnite and fluorite obtained in recent work on BaF_2.[12]

With a zero-pressure bulk modulus of 74(5) GPa, the cotunnite phase of CaF_2 is slightly more compressible than the fluorite phase. The same relationship was recently found between the cotunnite and fluorite phases of BaF_2 by Smith *et al.*[12] A previous static compression experiment[15] on CaF_2 yielded a much higher bulk modulus for the cotunnite phase ($K_0=170$ GPa). The presence of differential stress is known to lead to overestimation of the bulk modulus in static compression studies;[59] this is the most likely explanation for the discrepancy as the results of Ref. 15 were obtained from an unannealed sample in a methanol-ethanol medium at up to 45 GPa, well above the pressure limit of the hydrostaticity of this medium.[60] Similar results are found in the case of BaF_2, where a more recent experiment[12] conducted with a quasihydrostatic He pressure medium yielded a much lower bulk modulus for the cotunnite-type phase than earlier work of Leger *et al.*[16] with a silicone grease medium. For the cotunnite phase of SrF_2, fewer data and the narrower pressure stability range give a poorer constraint on K_0, but the fit is consistent with the trend seen in CaF_2 and BaF_2. The bulk modulus of 74(8) GPa is within uncertainty from the bulk modulus of the fluorite phase of SrF_2. The fit value of V_0 for the cotunnite phase yields a volume relative to the fluorite phase of $V_0(\text{cotunnite})/V_0(\text{fluorite})=0.90(1)$, which is lower than the values for either CaF_2 or BaF_2. If V_0 is fixed to a value of 150.5 Å^3 [$V_0(\text{cotunnite})/V_0(\text{fluorite})=0.92$ between the relative volumes for CaF_2 and BaF_2], then the fit value of K_0 becomes 62(1) GPa, between the K_0 values for CaF_2 and BaF_2.[12]

The similar compressibility of fluorite and cotunnite forms of CaF_2 is consistent with recent density-functional theory calculations,[5,10,11] for which generalized gradient approximation (GGA) calculation gives better quantitative agreement with K_0 than the local-density approximation.

TABLE III. Observed and calculated d spacings for the Ni_2In-type phase of CaF_2 at 92 GPa and 300 K. These peaks are fit to a hexagonal unit cell with $a=3.5230(5)$ Å, $c=4.4337(10)$ Å, and $V=47.66(2)$ Å^3.

h	k	l	d_{obs} (Å)	d_{calc} (Å)	Δd (Å)	Intensity (%)
1	0	0	3.05045	3.05104	−0.00059	9
1	0	1	2.51439	2.51342	0.00097	27
0	0	2	2.21665	2.21683	−0.00018	7
1	0	2	1.79308	1.79342	−0.00034	66
1	1	0	1.76184	1.76152	0.00032	100
2	0	1	1.44230	1.44252	−0.00022	6
2	0	2	1.25698	1.25671	0.00027	7

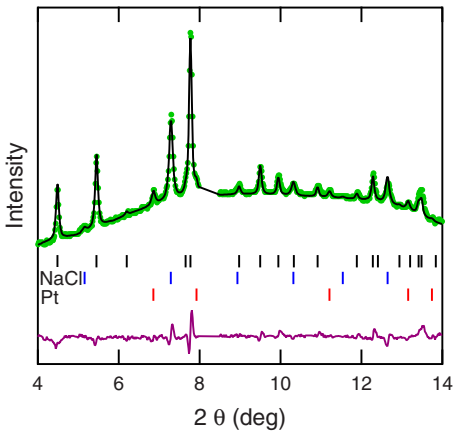

FIG. 4. (Color online) Full profile refinement of SrF_2 Ni_2In-type phase with $P6_3/mmc$ symmetry and atomic positions Sr: (1/3, 2/3, 1/4), F: (0, 0, 0), and (1/3, 2/3, 3/4). Refined fit curve is superimposed on measured intensities (dots), with the residual curve below. Vertical ticks mark peak positions for SrF_2 Ni_2In-type, NaCl B2, and Pt phases.

Other theoretical calculations for CaF_2 and SrF_2 suggest a much higher[6,7] bulk modulus for the cotunnite phase. The same has been found for BaF_2: the most recent calculations for BaF_2 using the GGA method yield a bulk modulus for the cotunnite-type phase in good agreement with experimental data obtained under hydrostatic conditions,[12] but earlier theoretical results using other techniques[8,9,18] predicted a higher bulk modulus. Experiments conducted under hydrostatic conditions and recent theoretical work thus appear to be converging on compressibility for the cotunnite-type phase comparable to that of the fluorite phase.

Figure 6 shows variation in lattice parameters with pressure for the cotunnite phases of CaF_2, SrF_2, and BaF_2. Near the upper pressure limit of the stability of the cotunnite-type phase, in well-annealed samples we observed a continuous change in the lattice parameters of the orthorhombic unit cell

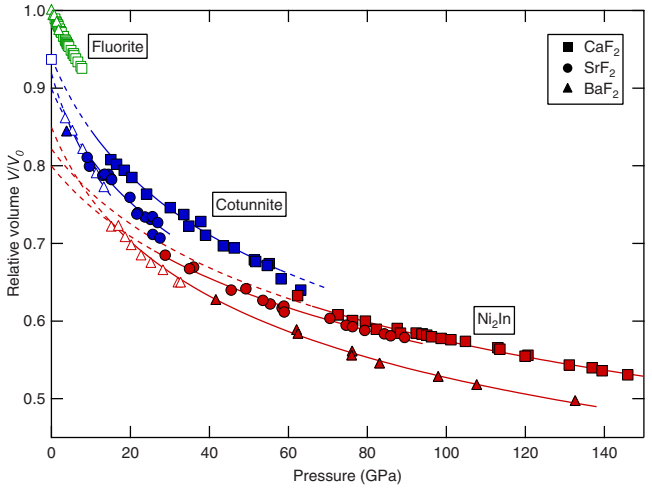

FIG. 5. (Color online) Compression curves and Birch-Murnaghan equation of state fits for CaF_2, SrF_2, and BaF_2. Open symbols are from previous experimental work (Refs. 4, 12, and 57). All data are plotted relative to V_0 of the fluorite phase.

with a discontinuous change in the axial compressibilities. Above 55 GPa, the c lattice parameter expands with increasing pressure, but a more rapid increase in compressibility of the a parameter results in a net increase in volumetric compressibility (Fig. 5). Figure 7 shows a direct comparison of interplanar spacings across the cotunnite-Ni_2In phase transition for the three alkaline earth fluorides. This phenomenon was also observed by Smith *et al.*[12] in BaF_2 and predicted by Ayala[18] in BaF_2 and Kunc *et al.*[61] in Li_2O (anticotunnite). Consistent with the group-subgroup relationship between the cotunnite and Ni_2In-type structures, we observe a continuous evolution of the orthorhombic structure toward the hexagonal structure near the phase transition. However, the hysteresis without laser heating and the 5% volume change with heating observed across the transition to the hexagonal phase for all three alkaline earth fluorides indicate that this phase transition is first order.

2. Ni_2In-type phase

Table V summarizes equation of state parameters for the Ni_2In phase of CaF_2, SrF_2, and BaF_2. The Ni_2In phase of BaF_2 is constrained over the widest range of experimental data from its transition pressure at 12 GPa (Ref. 16) to our maximum pressure of 133 GPa. The equation of state described by our annealed data (shown in Fig. 5) from 42–133 GPa matches well with the measurement in a He pressure medium by Smith *et al.* from 15–33 GPa: K_0 is 67(9) GPa and V_0 is 202(4) Å^3, 85% of the fluorite V_0. This bulk modulus is comparable to Smith *et al.*'s theoretical and experimental values[12] but significantly lower than values measured by Leger *et al.*[16] and earlier theoretical calculations.[8,9,18] The Ni_2In-type phase of BaF_2 has the same zero-pressure bulk modulus as the cotunnite-type phase within experimental error.

Because the Ni_2In-type phases of CaF_2 and SrF_2 are stable only at higher pressures and become amorphous or transform to the cotunnite-type phase upon decompression, the zero-pressure equation of state parameters for these phases are more difficult to constrain. A wide range of values for V_0, K_0, and K_0' reproduce the high-pressure data. Fitting results with either V_0 or K_0' fixed are shown in Table V. Constraints on V_0 and K_0' are based on theoretical work and analogous experiments on BaF_2. The choice of these constraints strongly controls K_0. It is difficult to compare fit values for V_0 or K_0 to theoretical work[5,10,11] as most studies do not report K_0'. Our fit for CaF_2 agrees with theoretical values for V_0 and K_0 only if K_0' is high, about 5.9. Our results for SrF_2 are not consistent with theoretical work.[6] Either K_0 or K_0' must be higher for the Ni_2In-type phase than the cotunnite phase to fit the CaF_2 and SrF_2 data, unlike BaF_2, for which neither K_0 nor K_0' were significantly different for the fluorite, cotunnite, and Ni_2In-type phases. Theoretical studies[5,6,10,11] did not predict an increase in bulk modulus for the Ni_2In-type phase; instead, the bulk modulus was predicted to be less than or similar to that of the cotunnite phase, as in BaF_2. The compositional trend in the zero-pressure bulk modulus roughly shows higher K_0 for smaller cations but cannot be unambiguously resolved due to the parameter trade-offs.

TABLE IV. Birch-Murnaghan equation of state parameters for fluorite and cotunnite phases of alkaline earth fluorides from this and previous studies. Moduli from Brillouin scattering and ultrasonic studies have been corrected from adiabatic to isothermal values. V_0 for fluorite-type CaF_2, SrF_2, and BaF_2 are 163.6 ± 0.2 Å^3, 195.7 ± 0.17 Å^3, and 238.3 ± 0.2 Å^3, respectively.

Reference	K_0(fluorite) (GPa)	K_0'(fluorite)	K_0(cotunnite) (GPa)	K_0'(cotunnite)	V_0(cotunnite)/V_0(fluorite)
			CaF_2		
This work			74 ± 5	4.7[a]	0.94 ± 0.01
X-ray diffraction:					
Ref. 4	81 ± 1.2	5.22 ± 0.35			
Ref. 15	87 ± 5	5 ± 1	169 ± 8 [b]	4.7[a,b]	0.86
Ref. 57					0.937
Brillouin scattering[22]	82.0 ± 0.7	4.83 ± 0.13			
Theory[5,7,10,11,19]	77–103	4–4.92	66–153.8	4.1–4.38	0.863–0.937
			SrF_2		
This work			74 ± 8	4.7[a]	0.90 ± 0.01
			62 ± 1	4.7[a]	0.92[a]
Ultrasonics[20,21]	70–71	4.76 ± 0.06			
Theory[6,7]	66–90		117–127		0.793–0.868
			BaF_2		
X-ray diffraction:					
Ref. 12			51 ± 4	4.7[a]	0.92 ± 0.01
Ref. 16			79 ± 10	4[a]	0.907 ± 0.005
Ultrasonics[23]	56.9				
Theory[8,9,12,18]	50–80	4.67–4.91	52–98	4.7[c]	0.876–0.937

[a]Parameter fixed in fit.
[b]Birch-Murnaghan equation fit to reported diffraction data.
[c]Only Ref. 12 provides a value for K_0'.

To more directly compare the compressibilities of CaF_2, SrF_2, and BaF_2 in the same pressure regime as our data, we examine the bulk modulus, K, calculated at high pressures. Differentiation of the Birch-Murnaghan equation yields a third-order finite strain expression of the variation in K with compression.[62] Results for the three compositions under consideration here are calculated with the parameters given in Table V with K_0' fixed at 4.7 and shown in Fig. 8. The change in bulk modulus is small across the fluorite-cotunnite transition for all compositions and suggests the cotunnite phase can be more compressible than the fluorite phase. In contrast, for the cotunnite-Ni_2In transition, there is a large increase in bulk modulus at the phase transition pressure. At the cotunnite-Ni_2In-type phase transition pressure of 14 GPa, the bulk modulus, K(14 GPa), is 10–30% larger for the Ni_2In-type phase than for the cotunnite phase. This is greater than the bulk modulus contrast calculated from the experimental equation of state of Ref. 12 (7%), although both this previous work and our equations of state have volume V(14 GPa) for the Ni_2In-type phase 5% lower relative to the cotunnite-type phase.[12] CaF_2 and SrF_2 also display a 5% volume reduction across the cotunnite-Ni_2In-type transition, although theoretical studies[5,6,10,11] predicted the volume change would be 0–2.5 % for these materials. For CaF_2 and SrF_2, the change in the bulk modulus across the transition is greater than for BaF_2: the cotunnite-Ni_2In-type transition results in a 20–40 % (CaF_2) to 45–65 % (SrF_2) increase in the bulk modulus. At 100 GPa, the Ni_2In-type phase has a bulk modulus of 240 GPa for BaF_2, 330 GPa for SrF_2, and 320 GPa for CaF_2. The higher bulk modulus values for SrF_2 relative to CaF_2 may reflect experimental uncertainty and require further investigation.

In previous experimental and theoretical studies on the Ni_2In-type phase of BaF_2,[12,16,18] an anomalously high value of the bulk modulus has been shown to be linked with a systematically high value of the c lattice parameter and hence c/a ratio. Leger *et al.*[16] observed an increase in the c/a ratio with pressure, but their pressure transmitting medium, silicone grease, is nonhydrostatic above 0.9 GPa.[60] Theoretical work[18] predicted a decrease in c/a ratio with pressure and suggested that differential stress resulted in the c lattice parameter being less compressible than under hydrostatic conditions. Recent x-ray diffraction experiments by Smith *et al.*[12] comparing quasihydrostatic compression in a He medium to nonhydrostatic compression with no pressure medium confirm this. Measured volumes in a nonhydrostatic

TABLE V. Birch-Murnaghan equation of state parameters for Ni_2In-type phases of alkaline earth fluorides from this and previous studies.

Reference	K_0 (GPa)	K_0'	$V_0(Ni_2In\text{-type})/V_0(\text{fluorite})$
		CaF_2	
This work	118 ± 11	4.7[a]	0.82 ± 0.01
	95 ± 5	5.1 ± 0.3	0.85[a]
	60 ± 5	5.9 ± 0.5	0.90[a]
Theory (Refs. 5, 10, and 11)	61–91	4.8[b]	0.890–0.925
		SrF_2	
This work	125 ± 9	4.7[a]	0.80 ± 0.01
	64 ± 5	7.0 ± 0.6	0.85[a]
	32 ± 4	10 ± 1.4	0.90[a]
Theory (Ref. 6)	43.8		0.633
		BaF_2	
This work	67 ± 9	4.7[a]	0.85 ± 0.02
X-ray diffraction			
Ref. 12	56 ± 5	4.67[a]	0.86 ± 0.02
Ref. 16	133 ± 16	4[a]	0.829 ± 0.012
Theory (Refs. 8, 9, 12, and 18)	69–142	4.67[c]	0.753–0.864

[a]Parameter fixed in fit.
[b]Only Ref. 11 provides a value for K_0'.
[c]Only Ref. 12 provides a value for K_0'.

sample were as much as 10% greater than in a quasihydrostatic sample, creating the appearance of a much less compressible phase. The volume difference between the two experiments is due almost entirely to the behavior of the c parameter.

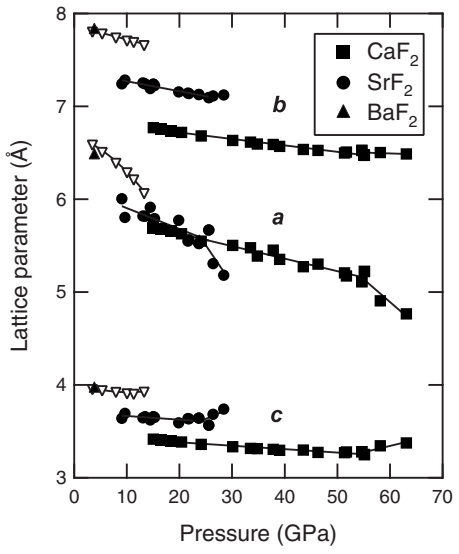

FIG. 6. Lattice parameters of the cotunnite-type phase of alkaline earth fluorides. Open triangles are from previous work in He medium (Ref. 12). Linear fits are shown as a guide to the eye. Near the upper stability limit, the structure distorts continuously toward the hexagonal phase: the a parameter becomes more compressible while c increases in magnitude.

In our experiments on all three compounds we find the c/a ratio of the Ni_2In-type phase decreased with pressure as long as the sample was well annealed (Fig. 9). The c/a ratio increased significantly if differential stress was allowed to accumulate. We heated our BaF_2 sample at approximately 10–15 GPa intervals. The c parameter appears less compressible in these intervals than immediately after heating, as can be observed from the open symbols in Fig. 9. The c/a ratio of the Ni_2In-type phase correlates well with diffraction peak widths and the normalized differential stress (t/P) measured in platinum (Fig. 10): the linear correlation coefficient $\rho = 0.69$. This correlation is strong enough to suggest that the c/a ratio of BaF_2 could be used to calibrate differential stress above 12 GPa. While the differential stress in Pt could not be measured in SrF_2 experiments above 60 GPa due to overlap between Pt and sample diffraction peaks, peaks were slightly wider in this experimental run than other well-annealed runs, which may indicate less hydrostatic conditions, resulting in a higher c/a ratio and volume. However, the decrease in c/a ratio with pressure measured in both CaF_2 and SrF_2 may be evidence that the bulk modulus has not been overestimated here due to differential stress.

Experimental data provide an important test for theoretical studies. Theoretical calculations for the alkaline earth fluorides have used a variety of techniques from atomistic to *ab initio* simulations involving different levels of sophistica-

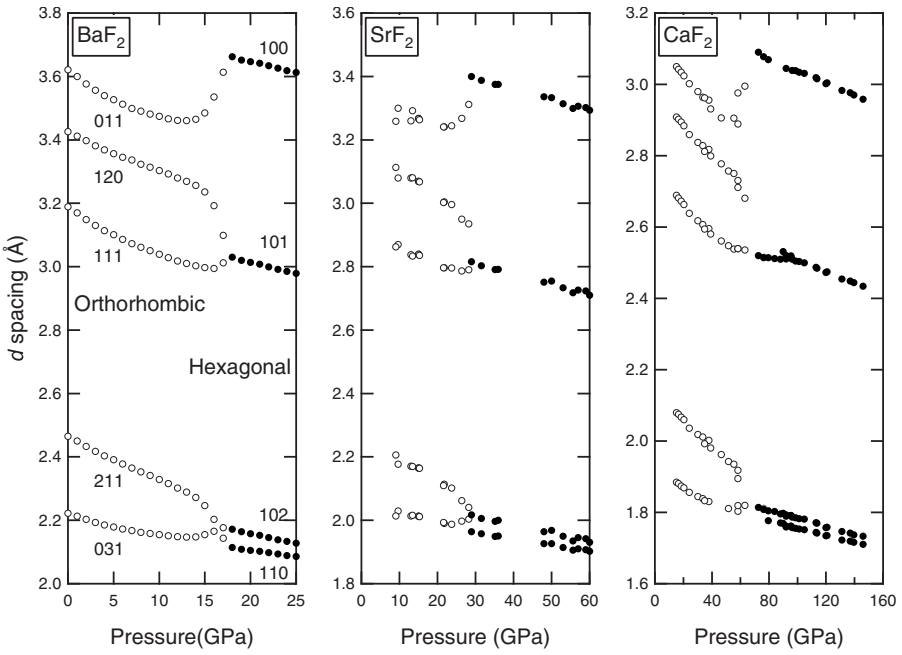

FIG. 7. Interplanar spacing variation across the cotunnite-Ni_2In transition. Open symbols represent cotunnite-type phase diffraction peaks. Closed symbols are Ni_2In-type phase peaks. CaF_2 and SrF_2 data are from this study. BaF_2 data are from molecular-dynamics simulation (Ref. 26).

tion. Among density-functional theory calculations, we find that results for CaF_2 by Wu *et al.*[5] using GGA most closely matched our transition pressures. However, studies using the GGA method have produced a wide range of pressures for the cotunnite-Ni_2In-type transition in CaF_2,[5,10,11] and all predict bulk moduli lower than those we observe for the Ni_2In-type phases of CaF_2 and SrF_2.[5,6,10,11] Theoretical studies on BaF_2 had previously reported zero-pressure bulk moduli for the Ni_2In-type phase of over 133 GPa,[8,9,18] until Smith *et al.*[12] reported an experimental value of 56 GPa and confirmed a higher compressibility with their own GGA calculations. This highlights the importance of experimental confirmation of theoretical predictions.

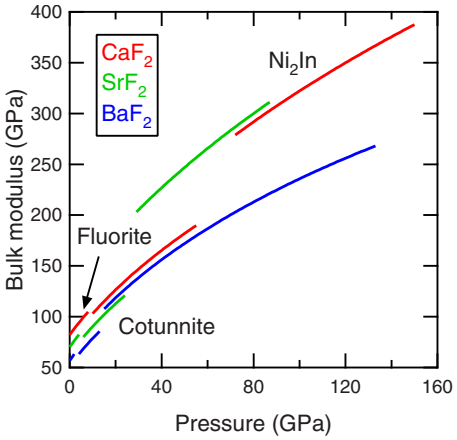

FIG. 8. (Color online) Bulk modulus vs pressure for CaF_2, SrF_2, and BaF_2 computed from Birch-Murnaghan equation of state fits to volume data. Gaps are left across phase transitions due to uncertainty in the compressibility in these regions.

IV. DISCUSSION

A. Static vs shock compression

CaF_2 and BaF_2 have both been examined to above 250 GPa using shock compression techniques.[37,58,63,64] These studies have identified phase transitions under dynamic loading and determined the equation of state along the Hugoniot. For both CaF_2 and BaF_2, x-ray examination of samples recovered from shock loading to 12–50 GPa showed partial transformation to the cotunnite-type phase.[58] The volume of the recovered cotunnite-type material was about 10% less than that of the fluorite phase, consistent with the static data reported in Table IV. In Fig. 11, Hugoniot data for CaF_2 (Refs. 37 and 63) and BaF_2 (Ref. 64) are plotted together with our and previous static measurements.[4,12] The shock data for CaF_2 at pressures below 100 GPa are qualitatively consistent with the transformation to the cotunnite-type phase: due to thermal effects along the Hugoniot, shock states lie at higher pressure (for a given volume) compared with static data. Below 25 GPa, the BaF_2 shock data similarly accord with the static data.

Above 100 GPa, the shock data suggest that CaF_2 transforms to a highly incompressible phase.[37] It was proposed that this change in compressibility is associated with a transformation to a phase with 11-fold or 12-fold coordination.[38,58] The transition to the Ni_2In-type phase occurs in CaF_2 at 72 GPa, which might be compatible with the shock data if the transition is kinetically delayed under dynamic loading. However, the comparison of our static compression data with the shock compression data (Fig. 11) shows that the Ni_2In-type phase is much more compressible than the observed shock compression data. Furthermore, the transition to the Ni_2In-type phase of BaF_2 near 14 GPa does not appear to be associated with an incompressible phase in shock or static data. Thus, the highly incompressible behavior in CaF_2 under shock loading cannot be linked with the

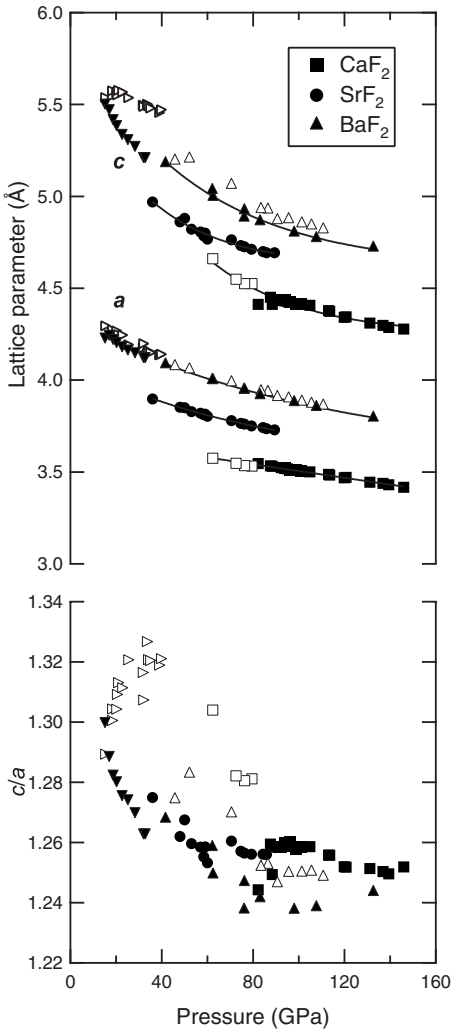

FIG. 9. Lattice parameters (upper panel) and c/a ratio (lower panel) for the Ni_2In-type phase of the alkaline earth fluorides. Filled symbols are for data under quasihydrostatic conditions while open symbols represent nonhydrostatic conditions. Open right-pointing triangles are from a nonhydrostatic experiment with a silicone grease medium (Ref. 16). Filled down-pointing triangles are from a hydrostatic experiment with a He medium (Ref. 12). In upper panel, least-squares fits are shown as a guide to the eye.

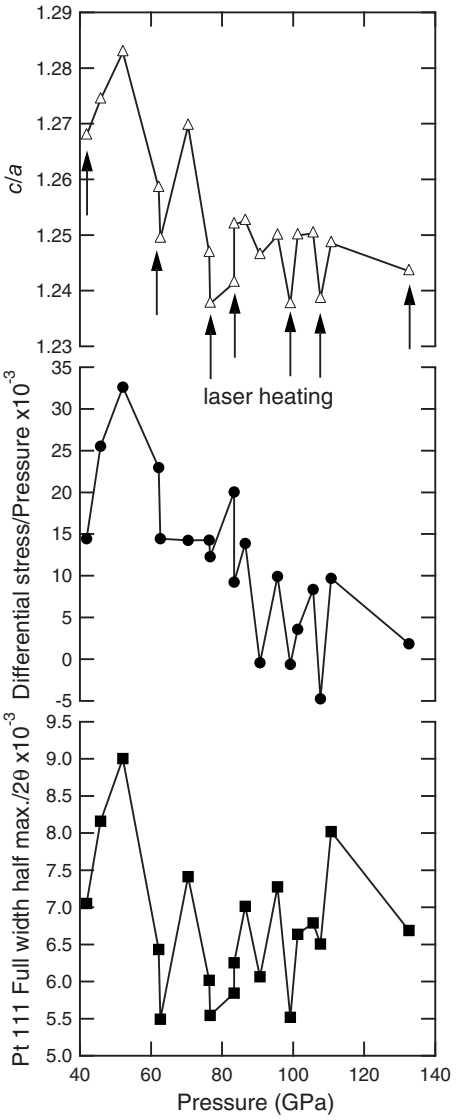

FIG. 10. For BaF_2, the c/a ratio of the Ni_2In-type phase (open triangles), the ratio of differential stress to pressure in Pt (filled circles), and the full width at half maximum for the Pt 111 peak normalized to the 2ϑ peak position (filled squares). The high degree of correlation (ρ=0.69) between the c/a ratio and these indicators of differential stress explains the systematic difference between measurements of this phase in different pressure media. Under nonhydrostatic conditions, the c/a ratio of this phase increases while under quasihydrostatic conditions (after laser annealing at pressures indicated by arrows) it decreases.

Ni_2In-type phase, which does not have a notably high bulk modulus (Table V, Fig. 8).

The shock compression data for BaF_2 (Ref. 64) do reveal similarly incompressible behavior above 100–150 GPa, the same or higher pressure than observed under shock loading in CaF_2. In our static experiments, we find no additional phase transitions in CaF_2 or BaF_2 in this pressure range to correspond with a highly incompressible phase, nor do we observe any additional high-temperature phases up to 3000 K. Whether additional phases appear in this system at the higher temperatures associated with shock loading is still unknown. The similarity of the pressures at which CaF_2 and BaF_2 become incompressible under shock loading suggest that, rather than a phase transition, thermal pressure may be responsible for the shock behavior of these compounds. Further shock compression studies of alkaline earth fluorides above 1 Mbar are needed to better understand their dynamic response, and efforts should also be directed to identification of other high-pressure solid or liquid phases that may be responsible for the observed behavior.

B. Phase-transition systematics

Figure 12 is a synthesis of the stable pressure ranges of known AF_2 phases from this and other experimental and theoretical studies.[5,16,65–71] The fluoride system exhibits a remarkably systematic dependence of the structure on pressure

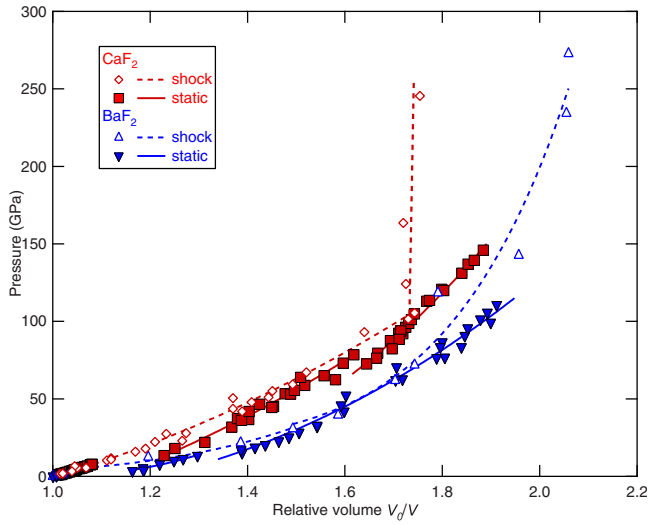

FIG. 11. (Color online) Shock compression data for CaF_2 (Refs. 37 and 63) (open diamonds) and BaF_2 (Ref. 64) (open up-pointing triangles) displayed with static data for CaF_2 [filled squares, this study and Angel (Ref. 4)] and BaF_2 [filled down-pointing triangles, this study and Smith *et al.* (Ref. 12)].

and atomic radius. This should be confirmed by further experimental study, particularly on ZnF_2, MnF_2, PdF_2, and CdF_2, none of which have been probed in the laboratory above 9 GPa.[66–68] The behavior of PbF_2 deviates from the alkaline earth fluorides: although the Ni_2In-type phase has been predicted by theory,[70] experiments found instead an isosymmetric transition to a Co_2Si-type structure.[71] This could possibly be due to the differences between the electronic structures of alkaline earth and transition-metal cations. As the evidence for an isosymmetric transition appears similar to the nonlinear compression behavior associated with the cotunnite-Ni_2In-type transition, further work should be undertaken to confirm whether Ni_2In-type PbF_2 can be synthesized.

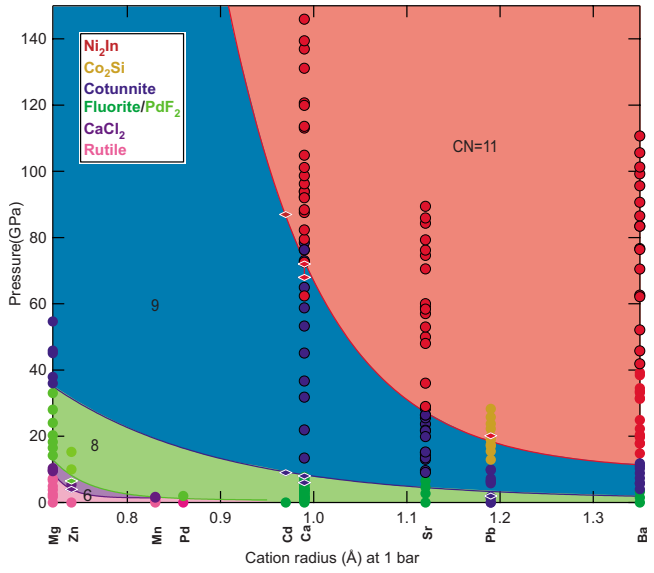

FIG. 12. (Color online) Phase stability range for fluoride compounds. Filled circles: experiment, diamonds: theory. Fluoride structures exhibit a systematic dependence on cation radius and pressure. CaF_2, SrF_2, and BaF_2 are constrained by this study (filled circles with black outlines). Other experimental data (filled circles without outlines) are from PdF_2 (Ref. 68), MnF_2 (Ref. 66), BaF_2 (Ref. 16), PbF_2 (Ref. 71), MgF_2 (Ref. 69), and ZnF_2 (Ref. 65). Transition pressures from theoretical calculations (diamonds) are shown for PbF_2 (Ref. 70), CaF_2 (Ref. 5), CdF_2 (Ref. 67), and ZnF_2 (Ref. 67).

A recent experiment[72] reported synthesis of an AlB_2-type phase with coordination number 12 in BaH_2 at 50–65 GPa. This phase then is a plausible candidate for a higher-pressure polymorph in the fluoride system. Based on cation radius considerations, BaF_2 would likely transform to this phase at the lowest pressure among fluorides. In addition, an insulator-metal transition[8] has also been predicted to occur in BaF_2. Recent theoretical calculations[12] predict the AlB_2 phase would not be stable below 250 GPa and the insulator-metal transition would occur above 500 GPa. Our experimental study demonstrates that no further structural transformation in BaF_2 occurs up to 133 GPa, and further experimental studies at ultrahigh pressures are necessary.

V. SUMMARY

To explore the systematic variation in phase-transition pressures and compressibility of high-pressure phases as a function of cation size for the alkaline earth fluorides, we performed x-ray diffraction experiments on CaF_2, SrF_2, and BaF_2 in the diamond-anvil cell at pressures up to 146 GPa, 89 GPa, and 133 GPa, respectively. These compounds undergo a common sequence of structural transitions from fluorite to cotunnite at 9 GPa, 5 GPa, and 3 GPa, respectively, and from cotunnite to Ni_2In-type structure at 72 GPa, 29 GPa, and 14 GPa, respectively. For all three fluorides, the zero-pressure bulk modulus of the cotunnite-type phase is the same or slightly less than that of the fluorite phase. At the transition pressure, the bulk modulus of the Ni_2In-type phase is more strongly dependent on cation size. While for BaF_2, the transition to the Ni_2In-type phase results in a 10–20 % increase in bulk modulus, for CaF_2 it increases the bulk modulus by 20–40 %. At 1 Mbar, the bulk moduli of the Ni_2In-type phases of CaF_2, SrF_2, and BaF_2 are 320 GPa, 330 GPa, and 240 GPa, respectively. Phase-transition pressures and bulk moduli for these high-pressure phases are within the wide range of theoretical predictions. Although the Ni_2In-type phase of CaF_2 had been suggested by dynamic compression results to be a possible ultra-incompressible material, our data do not support this.

The AF_2 system exhibits a systematic relationship between structure and cation/anion size ratio. Due to its large cation size and associated low phase-transition pressures, BaF_2 had been the only compound in the AF_2 system, demonstrated to transform to a Ni_2In-type phase. This work is an experimental confirmation of the Ni_2In-type structure in CaF_2 and SrF_2. AF_2 compounds with smaller cations than Ca, Sr, and Ba may undergo analogous cotunnite-Ni_2In-type transitions at higher pressures than those explored in this work. The Ni_2In-type structure may also be a common post-cotunnite phase among other AX_2 systems including materi-

als relevant to planetary science such as SiO_2 and possible superhard or super-incompressible materials such as TiO_2. Because the compressibility of the Ni_2In-type phase is more strongly dependent on cation than the cotunnite-type phase, further experimental work will be needed to determine the compressibility of Ni_2In-type phases in other systems.

ACKNOWLEDGMENTS

We thank Q. Guo, S.-H. Shim, and K. Catalli for experimental assistance and W. Nellis for helpful discussion. This work was supported by the NSF and the Carnegie-DOE Alliance Center. This work was performed at GeoSoilEnviroCARS (Sector 13) and High Pressure Collaborative Access Team (HPCAT, Sector 16) at the Advanced Photon Source (APS), Argonne National Laboratory, and beamline X17B3, National Synchrotron Light Source (NSLS), Brookhaven National Laboratory. GeoSoilEnviroCARS is supported by the NSF, DOE, and the State of Illinois. HPCAT is supported by DOE-BES, DOE-NNSA, NSF, and the W.M. Keck Foundation. Use of the APS and NSLS was supported by the U.S. Department of Energy, Office of Basic Energy Sciences. X17B3 is supported by the NSF Cooperative Agreement No. EAR 01-35554 to COMPRES (COnsortium for Materials Properties Research in Earth Sciences). Use of the National Synchrotron Light Source, Brookhaven National Laboratory, was supported by the U.S.-DOE under Contract No. DE-AC02-10886.

*Present address: Transnet Corporation.
†Present address: University of Texas, Austin.
‡Present address: Sumitomo Corporation.

[1] J. M. Leger and J. Haines, Eur. J. Solid State Inorg. Chem. **34**, 785 (1997).
[2] K. Kawano, T. Ohya, T. Tsurumi, K. Katoh, and R. Nakata, Phys. Rev. B **60**, 11984 (1999).
[3] R. M. Hazen and L. W. Finger, J. Appl. Crystallogr. **14**, 234 (1981).
[4] R. J. Angel, J. Phys.: Condens. Matter **5**, L141 (1993).
[5] X. Wu, S. Qin, and Z. Wu, Phys. Rev. B **73**, 134103 (2006).
[6] A.-m. Hao, X.-c. Yang, J. Li, W. Xin, S.-h. Zhang, X.-y. Zhang, and R.-p. Liu, Chin. Phys. Lett. **26**, 077103 (2009).
[7] V. Kanchana, G. Vaitheeswaran, and M. Rajagopalan, Physica B **328**, 283 (2003).
[8] V. Kanchana, G. Vaitheeswaran, and M. Rajagopalan, J. Alloys Compd. **359**, 66 (2003).
[9] H. Jiang, R. Pandey, C. Darrigan, and M. Rérat, J. Phys.: Condens. Matter **15**, 709 (2003).
[10] H. Shi, W. Luo, B. Johansson, and R. Ahujia, J. Phys.: Condens. Matter **21**, 415501 (2009).
[11] S. Cui, W. Feng, H. Hu, Z. Feng, and Y. Wang, Comput. Mater. Sci. **47**, 41 (2009).
[12] J. S. Smith, S. Desgreniers, J. S. Tse, J. Sun, D. D. Klug, and Y. Ohishi, Phys. Rev. B **79**, 134104 (2009).
[13] Z.-y. Zeng, X.-r. Chen, J. Zhu, and C.-e Hu, Chin. Phys. Lett. **25**, 230 (2008).
[14] A. Kavner, Phys. Rev. B **77**, 224102 (2008).
[15] L. Gerward, J. Staun Olsen, S. Steenstrup, M. Malinowski, S. Asbrink, and A. Waskowska, J. Appl. Crystallogr. **25**, 578 (1992).
[16] J. M. Leger, J. Haines, A. Atouf, O. Schulte, and S. Hull, Phys. Rev. B **52**, 13247 (1995).
[17] E. Francisco, M. A. Blanco, and G. Sanjurjo, Phys. Rev. B **63**, 094107 (2001).
[18] A. P. Ayala, J. Phys.: Condens. Matter **13**, 11741 (2001).
[19] A. M. Pendás, J. M. Recio, M. Flórez, V. Luaña, and M. Bermejo, Phys. Rev. B **49**, 5858 (1994).
[20] G. A. Samara, Phys. Rev. B **13**, 4529 (1976).
[21] S. Alterovitz and D. Gerlich, Phys. Rev. B **1**, 2718 (1970).
[22] S. Speziale and T. S. Duffy, Phys. Chem. Miner. **29**, 465 (2002).
[23] C. Wong and D. E. Schuele, J. Phys. Chem. Solids **29**, 1309 (1968).
[24] H. I. Smith and J. H. Chen, Bull. Am. Phys. Soc. **11**, 414 (1966).
[25] D. P. Dandekar and J. C. Jamieson, Trans. Am. Crystallogr. Assoc. **5**, 19 (1969).
[26] K.-F. Seifert, Ber. Bunsenges. Phys. Chem **70**, 1041 (1966).
[27] G. A. Kourouklis and E. Anastassakis, Phys. Rev. B **34**, 1233 (1986).
[28] L. S. Dubrovinsky, N. A. Dubrovinskaia, V. Swamy, J. Muscat, N. M. Harrison, R. Ahuja, B. Holm, and B. Johansson, Nature (London) **410**, 653 (2001).
[29] N. A. Dubrovinskaia, L. S. Dubrovinsky, R. Ahuja, V. B. Prakapenka, V. Dmitriev, H.-P. Weber, J. M. Osorio-Guillen, and B. Johansson, Phys. Rev. Lett. **87**, 275501 (2001).
[30] S. R. Shieh, A. Kubo, T. S. Duffy, V. B. Prakapenka, and G. Shen, Phys. Rev. B **73**, 014105 (2006).
[31] J. Haines, J. M. Leger, and O. Schulte, J. Phys.: Condens. Matter **8**, 1631 (1996).
[32] S. Desgreniers and K. Lagarec, Phys. Rev. B **59**, 8467 (1999).
[33] O. Ohtaka, H. Fukui, T. Kunisada, T. Fujisawa, K. Funakoshi, W. Utsumi, T. Irifune, K. Kuroda, and T. Kikegawa, Phys. Rev. B **63**, 174108 (2001).
[34] O. Ohtaka, H. Fukui, T. Kunisada, T. Fujisawa, K. Funakoshi, W. Utsumi, T. Irifune, K. Kuroda, and T. Kikegawa, J. Am. Ceram. Soc. **84**, 1369 (2001).
[35] S. Duclos, Y. K. Vohra, A. L. Ruoff, A. Jayaraman, and G. P. Espinosa, Phys. Rev. B **38**, 7755 (1988).
[36] A. R. Oganov, M. J. Gillan, and G. D. Price, Phys. Rev. B **71**, 064104 (2005).
[37] L. V. Al'tshuler, M. A. Podurets, G. V. Simakov, and R. F. Trunin, Sov. Phys. Solid State **15**, 969 (1973).
[38] W. J. Nellis and T. Petach, *Shock Compression of Condensed Matter-2007* (American Institute of Physics, New York, 2007), pp. 89–92.
[39] H.-y. Chung, M. B. Weinberger, J. B. Levine, A. Kavner, J. M. Yang, S. H. Tolbert, and R. B. Kaner, Science **316**, 436 (2007).
[40] R. Yu, Q. Zhan, and L. C. De Jonghe, Angew. Chem., Int. Ed. **46**, 1136 (2007).
[41] R. Ahuja and L. S. Dubrovinsky, High Press. Res. **22**, 429 (2002).
[42] Y. Al-Khatatbeh, K. K. M. Lee, and B. Kiefer, Phys. Rev. B **79**,

134114 (2009).
[43] D. Nishio-Hamane, A. Shimizu, R. Ahuja, K. Niwa, A. Sano-Furukawa, T. Okada, T. Yagi, and T. Kikegawa, Phys. Chem. Miner. **37**, 129 (2010).
[44] B. Kiefer and T. S. Duffy, J. Appl. Phys. **97**, 114902 (2005).
[45] M. Rivers, V. Prakapenka, A. Kubo, C. Pullins, C. M. Holl, and S. D. Jacobsen, High Press. Res. **28**, 273 (2008).
[46] Y. Meng, G. Shen, and H.-k. Mao, J. Phys.: Condens. Matter **18**, S1097 (2006).
[47] V. B. Prakapenka, A. Kubo, A. Kuznetsov, A. Laskin, O. Shkurikhin, P. Dera, M. L. Rivers, and S. R. Sutton, High Press. Res. **28**, 225 (2008).
[48] G. Shen, M. L. Rivers, Y. Wang, and S. R. Sutton, Rev. Sci. Instrum. **72**, 1273 (2001).
[49] A. P. Hammersley, S. O. Svensson, M. Hanfland, A. N. Fitch, and D. Häusermann, High Press. Res. **14**, 235 (1996).
[50] T. J. B. Holland and S. A. T. Redfern, Miner. Mag. **61**, 65 (1997).
[51] A. C. Larson and R. B. Von Dreele, Los Alamos National Laboratory Report No. LAUR 86–748, 2000 (unpublished).
[52] B. H. Toby, J. Appl. Crystallogr. **34**, 210 (2001).
[53] N. C. Holmes, J. A. Moriarty, G. R. Gathers, and W. J. Nellis, J. Appl. Phys. **66**, 2962 (1989).
[54] A. K. Singh, J. Appl. Phys. **73**, 4278 (1993).
[55] S.-H. Shim, T. S. Duffy, and G. Shen, Phys. Earth Planet. Inter. **120**, 327 (2000).
[56] E. Menéndez-Proupin and A. K. Singh, Phys. Rev. B **76**, 054117 (2007).
[57] E. Morris, T. Groy, and K. Leinenweber, J. Phys. Chem. Solids **62**, 1117 (2001).
[58] V. N. German, N. N. Orlova, M. N. Pavlovskii, L. A. Tarasova, and R. F. Trunin, Izv. Acad. Sci. USSR, Phys. Solid Earth **8**, 487 (1975).
[59] T. S. Duffy, G. Shen, D. L. Heinz, J. Shu, Y. Ma, H.-k. Mao, R. J. Hemley, and A. K. Singh, Phys. Rev. B **60**, 15063 (1999).
[60] R. J. Angel, M. Bujak, J. Zhao, G. D. Gatta, and S. D. Jacobsen, J. Appl. Crystallogr. **40**, 26 (2007).
[61] K. Kunc, I. Loa, and K. Syassen, Phys. Rev. B **77**, 094110 (2008).
[62] I. Jackson, Geophys. J. Int. **134**, 291 (1998).
[63] M. Hasegawa, K. Kondo, and A. Sawaoka, Jpn. J. Appl. Phys., Part 1 **23**, 20 (1984).
[64] R. F. Trunin, L. F. Gudarenko, M. V. Zhernokletov, and G. V. Simakov, *Experimental Data on Shock Compressibility and Adiabatic Expansion of Condensed Substances* (RFNC-VNIIEF, Sarov, Russia, 2001).
[65] K. Kusaba and T. Kikegawa, Solid State Commun. **145**, 279 (2008).
[66] M. Yamaguchi, T. Yagi, N. Hamaya, and T. Yagi, J. Phys. Soc. Jpn. **61**, 3883 (1992).
[67] X. Wu and Z. Wu, Eur. Phys. J. B **50**, 521 (2006).
[68] A. Tressaud, J. L. Soubeyroux, H. Touhara, G. Demazeau, and F. Langlais, Mater. Res. Bull. **16**, 207 (1981).
[69] J. Haines, J. M. Leger, F. Gorelli, D. D. Klug, J. S. Tse, and Z. Q. Li, Phys. Rev. B **64**, 134110 (2001).
[70] A. Costales, M. A. Blanco, R. Pandey, and J. M. Recio, Phys. Rev. B **61**, 11359 (2000).
[71] J. Haines, J. M. Leger, and O. Schulte, Phys. Rev. B **57**, 7551 (1998).
[72] K. Kinoshita, M. Nishimura, Y. Akihama, and H. Kawamura, Solid State Commun. **141**, 69 (2007).